One-dimensional Model of Cubic Hopping Rover

Jianxun Jiang*, Xiangyuan Zeng*,†,Shuquan Wang**

*School of Automation, Beijing Institute of Technology, Beijing 100081, China
E-mail: zeng@bit.edu.cn
**Key Laboratory of Space Utilization, Chinese Academy of Sciences, Beijing 100094, China

Abstract.
Due to the irregular gravity field and complex surface terrain, Asteroid surface exploration is challenging. Hopping is considered a more promising asteroid surface motion scheme. This paper designs and presents one-dimensional wheel pendulum model that can jump up, roll and keep one-side balance. The reaction wheel mounted on the protective plate is the power source of the system. The sudden braking of the reaction wheel with high speed causes one-dimensional wheel pendulum model to jump up. When the pendulum body approaches the central axis of the system with weak momentum, the Single Chip Micyoco exerts control signal on the motor to keep the system in one-side balance. In this paper, numerical simulations of the system are carried out. The experimental study indicates that the system has the characteristics of quick start, strong stability and excellent immunity.

Keywords: one-dimensional wheel pendulum model, jump up, one-side balance

1. INTRODUCTION

Traditional wheeled rovers are suitable for the large bodies, such as Moon and Mars, where the distribution of gravity is similar to the Earth's. Unlike large planetary bodies, the weak and irregular gravity field [1] of small bodies [2] surface limits the movement of rovers. In a microgravity environment, conventional wheeled vehicles can easily escape from the gravity field of asteroids [3] when traversing rough terrain [4]. At present, hopping is considered to be the most effective way to move on the surface of asteroids [5][6][7]. On December 3rd, 2014, JAXA successfully launched the spacecraft, Hayabusa 2 [8]. Drawing on previous experience, Hayabusa 2 successfully deployed the hopping rover, MASCOT [9]. The aim of the project is to explore the surface of the asteroid 162173, Ryugu [10] and take some samples back to Earth by 2020. Hedgehog [11] is a cubic hopping rover developed by NASA JPL and Stanford. It can roll for short distance and hop to long distance target.

The accidental bounce of Philae's landing [12] tells us that the development of microgravity rover is a challenging project. Only controllable performance can ensure the smooth completion of the task. This paper presents the model building, design, simulation and implementation of one-dimensional model of the microgravity rover. According to the principle of conservation of angular momentum [13], the system moves in one-dimensional direction by the cooperation of reaction wheel [14] and brake module. The model can achieve jump up, roll, one-side balance by applying control signal to motor. All functional modules (power module, drive module, brake module, control module) are encapsulated integrated. The integrated design not only improves the motion efficiency but also saves space.

The rest of this paper is organized as follows. Section 2 introduces dynamic model of the system. The design of one-dimensional wheel pendulum model is summarized in Section 3. Section 4 discusses the results of the simulation and the actual experiments. Section 5 concludes this paper.

2. MODEING

In this section, the dynamic modeling of two motion state (balance and jump up) of one-dimensional wheel pendulum model is introduced.

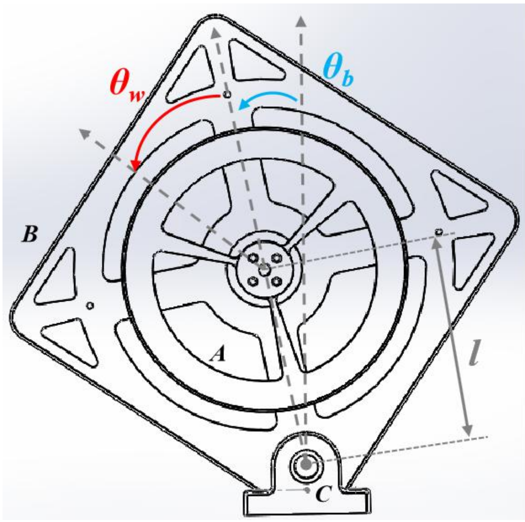

Fig. 1 The schematic diagram of one-dimensional wheel pendulum model.

Fig. 1 is a schematic diagram of a one-dimensional wheel pendulum model. The structure A is reaction wheel. The structure B is protective plate. The structure C is bearing base. A is driven by DC brushless motor. A and B can rotate together around the center of the bearing.

Notation :

- θ_b : The rotation angle of the pendulum body around the central axis of the system.
- θ_w : The rotation angle of the reaction wheel around the central axis of the pendulum body.
- L : The distance between centroid of system and center of bearing.
- m_{tot} : The total mass of pendulum body and reaction wheel.
- g : Gravitational acceleration.
- I_b : Moment of inertia of the pendulum body.
- I_w : Moment of inertia of the reaction wheel.
- F_b : Friction of the pendulum body.
- F_w : Friction of the reaction wheel.
- T_{motor}, τ : Torque output of motor .
- u : Input current of motor.
- K_m : motor constant.

2.1. Balance

The kinetic energy of the system is T, the potential energy is P. The Lagrange equation can be expressed as :

$$L = T - P \tag{1}$$

To solve the Lagrangian, the Euler-Lagrange equations is as follow :

$$\frac{d}{dt}\left(\frac{\partial L}{\partial \dot{\theta}}\right) - \frac{\partial L}{\partial \theta} + \frac{\partial R}{\partial \dot{\theta}} = \tau \tag{2}$$

τ is the torque generated by motor, $\frac{\partial R}{\partial \dot{\theta}}$ represents dissipative forces. As shown in **Fig. 2**, the potential energy P of the system can be formulated as:

$$P = l m_{tot} g \cos\theta_b \tag{3}$$

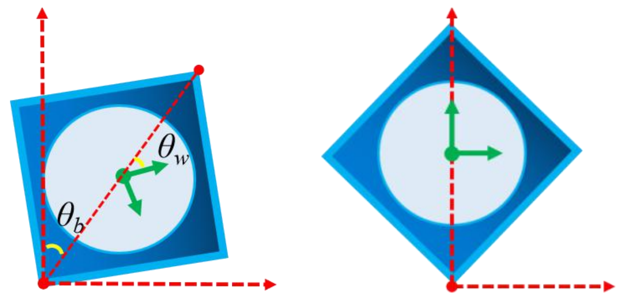

a.Instantaneous state *b*.Balance state

Fig. 2 Two motion states of one-dimensional pendulum wheel model

The kinetic energy T of the whole system is modeled as follow:

$$T = \frac{1}{2} I_b \dot{\theta}_b^2 + \frac{1}{2} I_w (\dot{\theta}_b + \dot{\theta}_w)^2 \tag{4}$$

Combining T and P the Lagrangian equation can be formulated as:

$$L = \frac{1}{2} I_b \dot{\theta}_b^2 + \frac{1}{2} I_w (\dot{\theta}_b + \dot{\theta}_w)^2 - L_t m_{tot} g \cos\theta_b \tag{5}$$

The generalized momenta is the derivatives of the Lagrangian with respect to angualr velocity. The following two equation are the derivatives of the generalized momenta with respect to time.

$$\frac{\mathrm{d}}{\mathrm{d}t}\left(\frac{\partial L}{\partial \dot{\theta}_b}\right) = I_b \ddot{\theta}_b + I_w \ddot{\theta}_w = M_{\theta_b} \tag{6}$$

$$\frac{\mathrm{d}}{\mathrm{d}t}\left(\frac{\partial L}{\partial \dot{\theta}_w}\right) = I_w\left(\ddot{\theta}_b + \ddot{\theta}_w\right) = M_{\theta_w} \tag{7}$$

Friction F_b, F_w and motor torque T_{motor} need to be added to obtain the derivative of Lagrange and state R with respect to angle.

$$\frac{\partial L}{\partial \theta_b} = L_t m_t g \sin\theta_b + F_b \dot{\theta}_b \tag{8}$$

$$\frac{\partial L}{\partial \theta_w} = T_{motor} - F_w \dot{\theta}_w \tag{9}$$

$$\frac{\partial R}{\partial \dot{\theta}_b} = F_b \dot{\theta}_b \tag{10}$$

$$\frac{\partial R}{\partial \dot{\theta}_w} = F_w \dot{\theta}_w \tag{11}$$

The following equation give the state R:

$$R = \frac{1}{2} F_b \dot{\theta}_b^2 + \frac{1}{2} F_w \dot{\theta}_w^2 \tag{12}$$

Combining with the equations above, the motion equations of the system can be formulated as:

$$\ddot{\theta}_b = \frac{L_t m_t g \sin\theta_b - T_{motor} + F_w \dot{\theta}_w - F_b \dot{\theta}_b}{I_b} \tag{13}$$

$$\begin{aligned} \ddot{\theta}_w &= \frac{T_{motor}(I_b + I_w) - F_w \dot{\theta}_w (I_b + I_w)}{I_b I_w} \\ &- \frac{L_t m_t g \sin\theta_b I_w + F_b \dot{\theta}_b I_w}{I_b I_w} \end{aligned} \tag{14}$$

The state space of the system can be obtained according to equation (13), (14). The state space model is defined as follows:

$$\begin{aligned} \dot{\boldsymbol{x}} &= A\boldsymbol{x} + B\boldsymbol{u} \\ \boldsymbol{y} &= C\boldsymbol{x} + D\boldsymbol{u} \end{aligned} \tag{15}$$

Define input variables for the system: $\left(\theta_b, \dot{\theta}_b, \dot{\theta}_w\right) = (0,0,0)$. The motor torque can be expresses by the current input.

$$T_{motor} = K_m u \tag{16}$$

The system matrices (A, B, C, D) are given by

$$A = \begin{bmatrix} 0 & 1 & 0 \\ \frac{L_t m_t g}{I_b} & \frac{-F_b}{I_b} & \frac{F_w}{I_b} \\ \frac{-L_t m_t g}{I_b} & \frac{-F_b}{I_b} & \frac{-F_w (I_b + I_w)}{I_b I_w} \end{bmatrix} \tag{17}$$

$$B = \begin{bmatrix} 0 \\ \dfrac{-K_m}{I_b} \\ \dfrac{K_m(I_b + I_w)}{I_b I_w} \end{bmatrix} \quad (18)$$

$$C = \begin{bmatrix} 1 & 0 & 0 \\ 0 & 1 & 0 \\ 0 & 0 & 1 \end{bmatrix} \quad (19)$$

$$D = [0] \quad (20)$$

2.2. Jump up

According to the law of conservation of angular momentum, the sudden braking of the reaction wheel at high speed will cause the whole system 'jump up'. As shown in **Fig. 3**, the complete jump up is the process of flipping from the stationary state to the one-sided balance position.

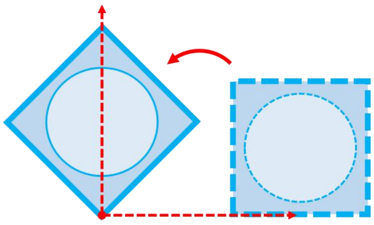

Fig. 3 The complete jump up process

According to the law of conservation of angular momentum, the reaction wheel with high speed rotation is break quickly, and the whole system will rotate around the center of bearing. It can be seen that the angular velocity of the reaction wheel is the key to determine the swing height of the system.

$$I_w \omega_w = (I_w + I_b + m_w l^2)\omega_b \quad (21)$$

The energy change of the system from stationary state to one-sided balance position:

$$\frac{1}{2}(I_w + I_b + m_w l^2)\omega_b^2 = (m_b l_b + m_w l)g(1 - \frac{1}{\sqrt{2}}) \quad (22)$$

Eliminating w_b from both equations gives

$$\omega_w^2 = (2 - \sqrt{2})\frac{(I_w + I_b + m_w l^2)}{I_w^2}(m_b l_b + m_w l)g \quad (23)$$

3. MODEL DESIGN

In this section, the structural design of one-dimensional wheel pendulum model is introduced. A side view of the system model is shown in **Fig. 4**,

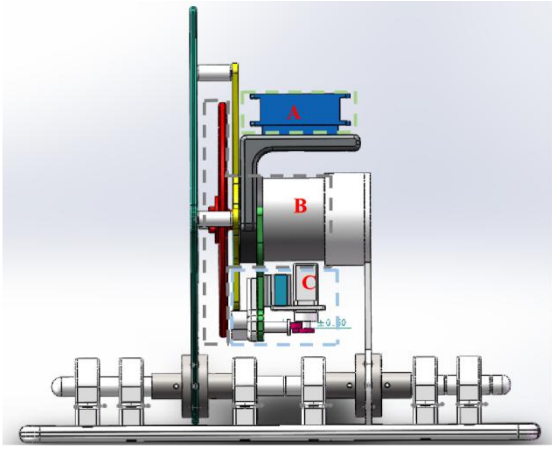

Fig. 4 A side view of the one-dimensional wheel pendulum

The key modules in the system have been marked with dotted boxes: A. Control module, B. Drive module, C. Brake module.

The control module is mainly composed of Stm32 Single Chip Micocomputer (SCM) and MPU6050 attitude sensor. The SCM controls the jump up and balance of the system by controlling the drive module and the brake module. MPU6050 collects the gyroscope and accelerometer to adjust the attitude of the system in real time.

A 20W DC brushless motor, reaction wheel and photoelectric encoder constitute the drive module of the system. DC brushless motor drive reaction wheel rotation and provide power for the system. The reaction wheel swing left and right to maintain the stability during the gradual balance of the system. The encoder transmits the rotation rate to SCM. Therefore, the speed of brushless motor can be regulated and controlled by the controller. A larger driving force can be obtained by appropriately increasing the mass of the reaction wheel.

The brake module consists of large metal steering gear, small bearing, light brake pad and spring. The combination of steering gear and break pad makes the reaction wheel brake instantly. The spring can quickly restore the brake pad to the initial position. The bearing is mounted on the rocker arm of the steering gear to make the force on the contact part more uniform.

The following table shows all the parameters of the one-dimensional wheel pendulum model.

Table 1. The parameters of the system

Variable	*Numerical Value*
l	0.085m
m_b	0.42kg
m_w	0.21kg
I_b	1.6×10^{-3} kg· m^2
I_w	0.38×10^{-3} kg· m^2
F_b	1.0×10^{-3} N
F_w	0.5×10^{-3} N
K_m	$25.1 \times$ N· m· A^{-1}

4. SIMULATION AND EXPERIMENTAL STUDY

This section designs a double closed loop PID controller for one-dimensional wheel pendulum. MATLAB/Simulink software is used to simulate, and the corresponding simulation results are obtained. We have completed the construction of the experimental platform. Moreover, use the upper computer to output the curve of key parameters with time.

4.1. Simulation

The PID controller is a linear controller constitutes a control deviation $e(t)$ according to the given value $r(t)$ and the actual output value $y(t)$.

$$e(t) = r(t) - y(t) \tag{24}$$

The control object is controlled by a linear combination of the proportion (P), integral (I) and differential (D) of the deviation. The control rule is formulates as:

$$u(t) = K_p \left[e(t) + \frac{1}{T_I}\int_0^t e(t)dt + T_D \frac{de(t)}{dt} \right] \tag{25}$$

The double closed loop PID controller is designed based on state space (A, B, C, D). The simulation schematic can be seen in **Fig. 5**.

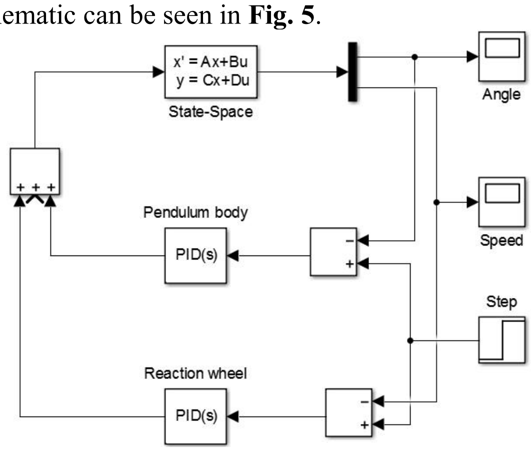

Fig. 5 The simulation Schematic of one-dimensional wheel pendulum model

Fig. 6 and **7** show the change of pendulum body angle and reaction wheel rotation rate with time in 50s.

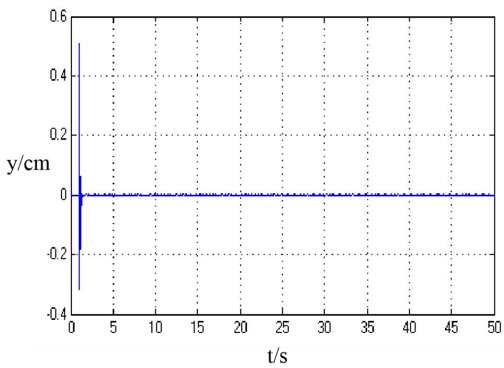

Fig. 6 Changes of pendulum body angle with time

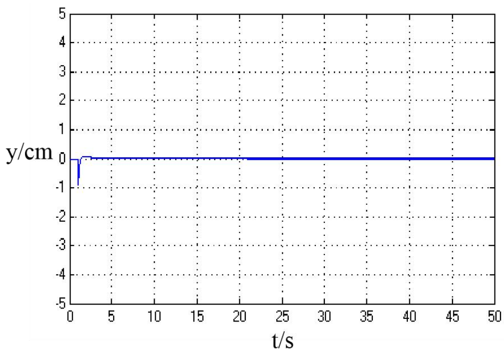

Fig. 7 Rotation speed of the reaction wheel versus time

The process of state adjustment ends in almost three seconds. According to the performance of the pendulum body after five seconds, it can be seen that the system has a high stability.

4.2. Final Product and Experiments

The experimental platform of one-dimensional wheel pendulum model is displayed in **Fig. 8**. Metal and 3-D print structure for the whole system ensures superior protection and support. The use of copper column connections between the protective front plate and the motor support not only reduces the system quality but also maintains the overall frame strength. A bearing block is used at the junction between the pendulum body and the bottom plate. This design gives the system excellent flexibility and reduces friction resistance at the contact site.

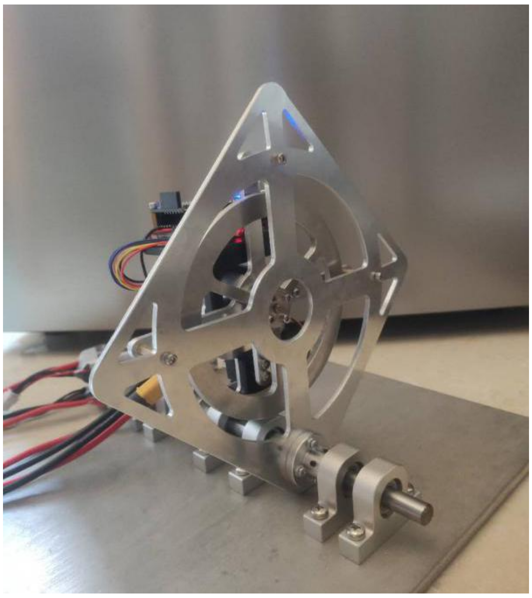

Fig. 8 one-dimensional wheel pendulum model in balance

In the actual experiment, the curve of the system swing angle and the reaction wheel speed with time can be seen in **Fig. 9** and **10**.

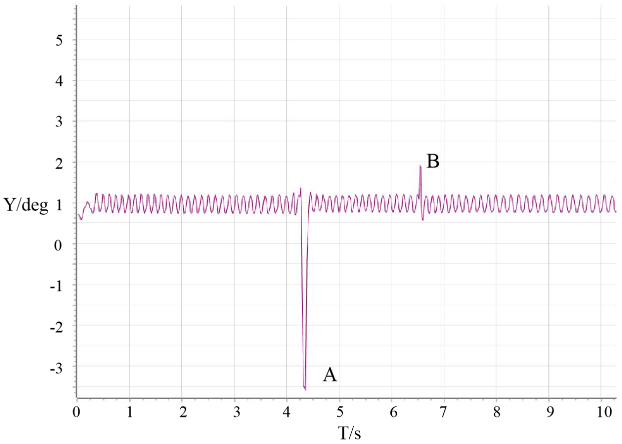

Fig. 9 Changes of the system swing angle with time

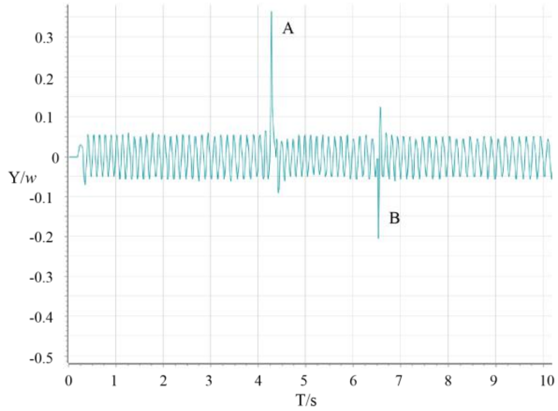

Fig. 10 Changes of the reaction wheel speed with time

Due to mechatronics, the mechanical equilibrium point of the system is 1^{o}. It can be seen from the output curve that the one-dimensional wheel pendulum model has extremely high stability. External disturbances are added at A B moment, and the system can be quickly restore to balance. it indicates that the system has strong disturbance rejection performance and fast response.

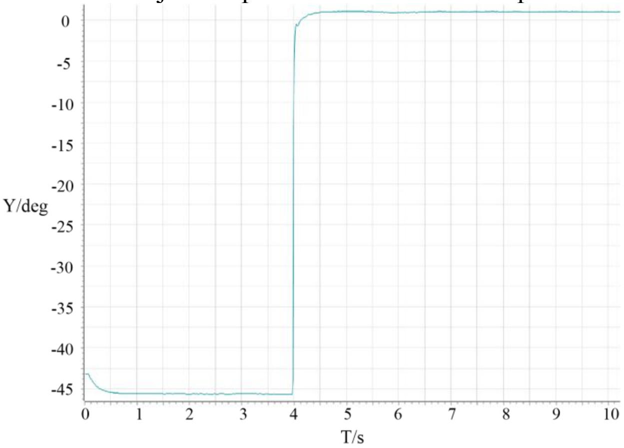

Fig. 11 One-dimensional wheel pendulum model keep one-side balance after braking

In **Fig. 11**, The system reach one-side balance rapidly after braking in a stationary state. In this work, the extremely high braking efficiency ensures that the system can reach the one-side balance position in a short time.

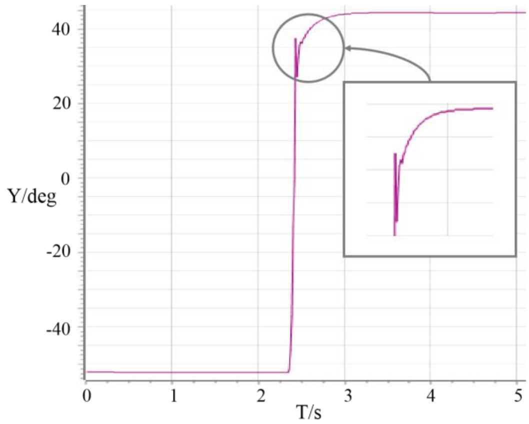

Fig. 12 The system rolls around the center of bearing

A whole roll procedure is shown in **Fig. 12**, where the brake action starts at 2.3 s. The system is basically balanced in 3 seconds. The magnification on the right side of **Fig. 12** shows the subsequent motion of the system at the end of the roll. The presence of a cushioning sponge can effectively reduce the impact between the pendulum body and the base. Eventually, after a collision, the angle of the system tends to flatten.

5. CONCLUSION

In order to adapt to the irregular and weak gravity environment of the asteroid surface exploration mission, this paper proposes and designs a one-dimensional wheel pendulum model. The system can roll and jump up by using a self-generated impact. Due to the exchange of angular momentum, the system can achieve one-side balance. The experimental behaviors are positively correlated with the simulation results. In addition, the real experiment shows the characteristics of rapid response, strong robustness and high brake efficiency. In the future, three-dimensional models will be designed to obtain a broader degree of freedom for motion.

Acknowledgements

This work was supported by the National Natural Science Foundation of China (No. 11972075). The Open Research Fund of Key Laboratory of Space Utilization and the Strategic Priority Research Program on Space Science, Chinese Academy of Sciences (No. LSU-KFJJ-2018-01) was also acknowledged.

REFERENCES:

[1] Y. Takahashi, D. J. Scheeres, R. A. Werner, "Surface gravity fields for asteroids and comets," Journal of guidance, control, and dynamics, 2013, 36 (2): 362-374.

[2] W. R. Wu, W. W. Liu, D. Qiao, D. G. Jie, "Investigation on the development of deep space exploration," Science China Technological Sciences, 2012, 55 (4): 1086-1091.

[3] B. Hockman, M. Pavone, "Stochastic motion planning for hopping rovers on small solar system bodies," [M]//Robotics Research, Springer, Cham, 2020, 877-893.

[4] T. M. Howard, A. Kelly, "Optimal rough terrain trajectory generation for wheeled mobile robots," The International Journal of Robotics Research, 2007, 26(2): 141-166.

[5] M. Pavone, J. C. Castillo-Rogez, I. A. D. Nesnas, J. A. Hoffman, N. J. Strange, "Spacecraft/rover hybrids for the exploration of small solar

system bodies," 2013 IEEE Aerospace Conference, IEEE, 2013, 1-11.

[6] T. G. Wen, X. Y. Zeng, C. Circi, Y. Gao, "Hop Reachable Domain on Irregularly Shaped Asteroids," Journal of Guidance, Control, and Dynamics,2020, 43(7): 1269-1283.

[7] J. X. Jiang, X. Y. Zeng, D. Guzzetti, Y. Y. You, "Path planning for asteroid hopping rovers with pre-trained deep reinforcement learning architectures," Acta Astronautica, 2020, 171: 265-279.

[8] S. Watanabe, Y. Tsuda, M. Yoshikawa, S. Tanaka, T. Saiki & S. Nakazawa, "Hayabusa2 mission overview," Space Science Reviews, 2017, 208(1-4): 1-14.

[9] M. Grott, J. Knollenberg, B. Borgs, F. Hänschke, E. Kessler, J. Helbert, A. Maturilli, N. Müller, "The MASCOT radiometer MARA for the Hayabusa 2 mission," Space Science Reviews, 2017, 208(1-4): 413-431.

[10] D. Perna, M. A. Barucci, M. Ishiguro, A. Alvarez-Candal, D. Kuroda, M. Yoshikawa, M.-J. Kim, S. Fornasier, S. Hasegawa, D.-G. Roh, T. G. Müller and Y. Kim, "Spectral and rotational properties of near-Earth asteroid (162173) Ryugu, target of the Hayabusa2 sample return mission," Astronomy & Astrophysics, 2017, 599.

[11] B. J. Hockman, A. Frick,R. G. Reid, I. A. Nesnas, M. Pavone, "Design, control, and experimentation of internally ‐ actuated rovers for the exploration of low ‐ gravity planetary bodies," Journal of Field Robotics, 2017, 34(1): 5-24.

[12] L. Witte, R. Roll, J. Biele, S.Ulamec, "Rosetta lander Philae–Landing performance and touchdown safety assessment," Acta Astronautica, 2016, 125: 149-160.

[13] K. Y. Bliokh, Y. P. Bliokh, "Conservation of angular momentum, transverse shift, and spin Hall effect in reflection and refraction of an electromagnetic wave packet," Physical review letters,2006, 96(7): 073903.

[14] D. J. Block, K. J. Åström, M. W. Spong, "The reaction wheel pendulum," Synthesis Lectures on Control and mechatronics, 2007, 1(1): 1-105.